PHYSICAL REVIEW A **84**, 030301(R) (2011)

Quantum-state tomography of a single nuclear spin qubit of an optically manipulated ytterbium atom

Atsushi Noguchi,[1,2] Yujiro Eto,[2] Masahito Ueda,[2,3] and Mikio Kozuma[1,2,*]

[1]*Department of Physics, Tokyo Institute of Technology, 2-12-1 O-okayama, Meguro-ku, Tokyo 152-8550, Japan*

[2]*ERATO Macroscopic Quantum Control Project, JST, 2-11-16 Yayoi, Bunkyo-Ku, Tokyo 113-8656, Japan*

[3]*Department of Physics, University of Tokyo, Hongo, Bunkyo-ku, Tokyo 113-0033, Japan*

(Received 8 June 2010; published 9 September 2011)

A single Yb atom is loaded into a high-finesse optical cavity with a moving lattice, and its nuclear spin state is manipulated using a nuclear magnetic resonance technique. A highly reliable quantum state control with fidelity and purity greater than 0.98 and 0.96, respectively, is confirmed by the full quantum state tomography; a projective measurement with high speed (500 μs) and high efficiency (0.98) is accomplished using the cavity QED technique. Because a hyperfine coupling is induced only when the projective measurement is operational, the long coherence times ($T_1 = 0.49$ s and $T_2 = 0.10$ s) are maintained.

DOI: 10.1103/PhysRevA.84.030301 PACS number(s): 03.67.Lx, 03.65.Wj, 32.80.−t, 42.50.Dv

It is advantageous to implement a qubit with a single nuclear spin [1–5] because the nuclear spin is robust against a stray magnetic field. This robustness can be attributed to the smallness of the magnetic moment of the nuclear spin as compared with that of the electronic spin [6]. It is essential to control a long-lived qubit with high fidelity for implementing complicated tasks of quantum information processing such as a quantum node of quantum telecommunication, scalable quantum computing, and quantum simulation.

Here, we provide a combination of techniques for a potential quantum information system. We employ a single nuclear spin of a ^{171}Yb atom in the form of a qubit in an optical lattice potential and implement both manipulation and state verification of the qubit with high fidelity and purity using nuclear magnetic resonance (NMR) and cavity QED techniques. Fidelity higher than 0.98 is obtained for the typical spin states including a superposition state, where the projective measurement is accomplished in 500 μs. While better fidelity (0.994) and detection speed (85 μs) have recently been demonstrated by using a similar cavity-neutral atom setup [7], the hyperfine state of an alkali-metal atom is utilized, and the system is not robust against a residual magnetic field [8].

It should be noted that a long coherence time of our qubit originates from an extremely weak coupling between the nuclear spin and the electromagnetic field, and that it is normally traded off for enabling fast and highly efficient state measurement. We couple the electronic spin with the nuclear spin using a hyperfine interaction in an excited state, and such a coupling is induced only when we irradiate the atoms with the probe light used for readout. We can thus achieve a long coherence time of the qubit with a fast and efficient detection of the state.

Our experimental setup, relevant energy levels, and the time chart of the experiment are shown in Fig. 1. We construct a qubit with a 1/2 nuclear spin of the ground state $^1S_0(F = 1/2)$ of the ^{171}Yb atom and define the quantized axis along the cavity axis by using the bias magnetic field induced by "Coil1." In the following discussion, $|\uparrow\rangle$ and $|\downarrow\rangle$ represent the magnetic sublevels of $^1S_0(F = 1/2)$. Details of Zeeman slowing and the double Magneto-Optical Trapping (MOT) system have been described in Refs. [9] and [10].

To load the atoms into the cavity mode, we utilize a "moving lattice." We first activate an optical standing wave potential, which is created by counterpropagating frequency-doubled YVO_4 laser beams (532 nm) with a peak potential depth of 110 μK. Because the optical standing wave overlaps the MOT beams, atoms are loaded to the lattice potential. After the MOT beams and the relevant magnetic field are turned off, the lattice potential starts moving with a speed that is proportional to the relative frequency difference δ between two counterpropagating beams. By changing the value of δ according to the relation $\delta(t) = \delta_0 \sin(\pi t/\tau)$, atoms are transported to the cavity mode, where $\delta_0 = 2\pi \times 700$ kHz and $\tau = 100$ ms. To initialize the nuclear spin state to $|\downarrow\rangle$, we irradiate the atoms in the moving lattice with a circularly polarized spin polarization beam that is resonant with the $^1S_0(F = 1/2) \rightarrow {}^1P_1(F' = 1/2)$ transition (399 nm). When we manipulate the nuclear spin state, the radiofrequency (rf) of the magnetic field is applied to the atoms by using "Coil2" after the atoms enter the cavity mode, where the radiofrequency is resonant with the Zeeman splitting between two substates $|\uparrow\rangle$ and $|\downarrow\rangle$ [Fig. 1(a), $\delta_g = 2\pi \times 2.5$ kHz]. Because of the rf irradiation, the nuclear spins in the atoms rotate around the axis orthogonal to the cavity axis. Our cavity consists of two concave mirrors having ultrahigh reflectivity at 556 nm and is characterized by the following three parameters: the maximum interaction rate between atoms and photons $g_0 = 2\pi \times 2.8$ MHz, the cavity decay rate (half-width half maximum, HWHM, of the cavity resonance line) $\kappa = 2\pi \times 4.8$ MHz, and the atom decay rate (half natural linewidth) $\gamma = 2\pi \times 91$ kHz. The length of our cavity is stabilized to 150 μm by injecting a 560 nm laser beam and utilizing the Frequency Modulation (FM) side-band method such that the cavity is resonant with the $^1S_0(F = 1/2) \rightarrow {}^3P_1(F' = 3/2)$ transition (556 nm). It should be noted that the far-off resonant locking beam (560 nm) is responsible for trapping the atoms in the cavity mode, where the trap depth is 30 μK (the beam waist is 19 μm).

*kozuma@ap.titech.ac.jp

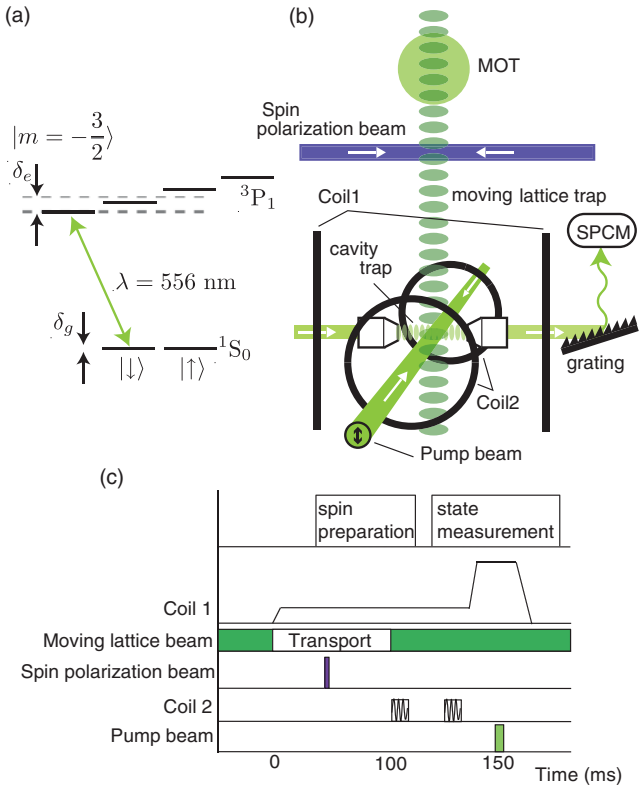

FIG. 1. (Color online) Experimental setup and time chart. (a) Energy-level diagram of ^{171}Yb. (b) Experimental setup. (c) Time chart for experiment. $|\uparrow\rangle$ and $|\downarrow\rangle$ denote the magnetic sublevels $m_F = +1/2$ and $-1/2$ in the ground state $^1S_0(F = 1/2)$, respectively. The substates in the excited state $^3P_1$ are labeled as $|m_F\rangle$.

To perform the projective measurement, we increase the bias magnetic field and the Zeeman splitting in the excited state $^3P_1(F' = 3/2)$, where the splitting $\delta_e = 2\pi \times 60$ MHz is much larger than the cavity-enhanced linewidth $\Gamma = \gamma[1 + 2g^2/(\kappa\gamma)] = 2\pi \times 3.4$ MHz for the $^1S_0(F = 1/2) \rightarrow {}^3P_1(F' = 3/2)$ transition. When the atoms are irradiated with a linearly polarized pump beam resonant with the $^1S_0(F = 1/2) \rightarrow {}^3P_1(F' = 3/2)$ transition, only the $|\downarrow\rangle$ atoms are excited in a cyclic manner and repeatedly emit fluorescence photons into the cavity mode. Therefore, the detection of more than one photon implies that the nuclear spin is projected to $|\downarrow\rangle$.

To perform experiments with single atoms, we prepare dilute atoms such that the expected mean atom number in the cavity mode becomes less than unity. The total detection efficiency of a photon emitted from an atom is 0.1; this value is enhanced by the Purcell effect. We obtain four photons from each single atom on average. On the basis of the assumption of the binomial distribution for photodetection, the efficiency of the projective measurement is estimated to be 0.98. The result obtained from the projective measurement contain errors that can be attributed to the dark counts of the detector and also to unwanted spin flips caused by the excitation of the $|\uparrow\rangle$ state. These lead to about 2% error for the diagonal elements of the density matrix.

The time chart [Fig. 1(c)] of the experiment consists of two parts (i.e., the preparation and detection of the nuclear

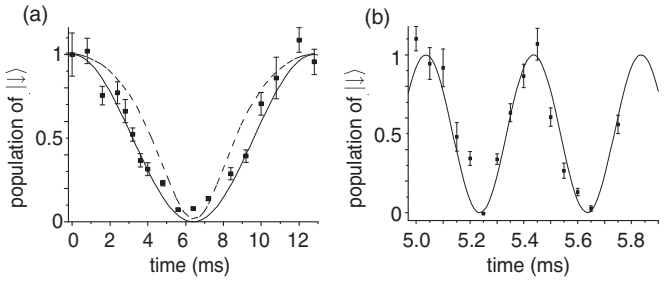

FIG. 2. Rabi oscillation and Ramsey interference. Time developments of population of $|\downarrow\rangle$ state as measured by (a) Rabi oscillation and (b) Ramsey interference. The error bars are estimated on the basis of the statistical distribution of signal counts. The solid (dotted) curve is a fit based on the assumption that there is a single atom (two atoms) in the cavity mode.

spin states). Arbitrary single nuclear spin states are prepared by rotating nuclear spins around two orthogonal axes. The rotation around the cavity axis is accomplished using the Larmor precession generated by the bias magnetic field, and the other rotation is implemented using Rabi oscillations through irradiation of the resonant rf field. Figure 2(a) shows the Rabi oscillations of the single nuclear spin generated by the rf field. We induce Zeeman splitting between the two ground states $|\uparrow\rangle$ and $|\downarrow\rangle$ using the bias magnetic field and apply a square-shaped rf pulse whose frequency is resonant with the splitting $\delta_g = 2\pi \times 2.5$ kHz. The population of the down spin state as a function of the rf irradiation time is shown in Fig. 2(a). Experimental results show a visibility of 0.96, which is estimated by sinusoidal fitting. This high visibility enables us to precisely control the nuclear spin rotation around one axis. The fact that the operation is carried out using single nuclear spins can be confirmed as follows: In our projective measurement, we consider that the spin is projected to $|\downarrow\rangle$ when the photodetector counts more than one photon. Suppose that there are two atoms in the cavity mode. In this case, the photon counts are obtained even if the spin state is $|\downarrow\downarrow\rangle$, $|\downarrow\uparrow\rangle$, or $|\uparrow\downarrow\rangle$; thus, the variation in the probability of detecting more than one photon is no longer sinusoidal [see the dotted curve in Fig. 2(a)]. The mean squared error is estimated to be $2.2 \times 10^{-4}(1.5 \times 10^{-3})$ with respect to the theoretical curve based on the assumption that there exists a single atom (two atoms) in the microcavity. The curve obtained from the experimental results represents a simple sinusoidal curve, which indicates the successful postselection of a single nuclear spin.

To check the controllability of two-axis rotations, we measure the Ramsey interference for a single nuclear spin. On the basis of the measurements of the Rabi oscillations [Fig. 2(a)], we use an rf field with a duration of 3.2 ms as a $\pi/2$ pulse. We irradiate single nuclear spins with two $\pi/2$ rf pulses, and the nuclear spins rotate around the cavity axis during the interval between the two pulses. The population of the down-spin state as a function of the time interval between the two rf pulses is shown in Fig. 2(b). The curve obtained from the experimental results is in good agreement with the theoretical curve, and the visibility is calculated from the sinusoidal fitting to be 0.99, which is consistent with the value expected from the error generated in the

projective measurement. It should be noted that the obtained visibility of Ramsey interference (0.99) is slightly higher than that obtained from the Rabi oscillations. In our experiment, the stability of the bias magnetic field is better than that of the rf field. We believe that the above difference arises because the rf irradiation time in the case of the Ramsey interference experiment is shorter than that in the case of the Rabi oscillation experiment. Hereafter, we use only $\pi/2$ pulses of the rf field. By appropriately varying the timing of the $\pi/2$ pulses, superposition states and also eigenstates are prepared.

By using spin polarization and rotation, we prepare arbitrary states of single nuclear spins. Here, three typical spin states are prepared; namely, (a) $(|\uparrow\rangle + |\downarrow\rangle)/\sqrt{2}$, (b) $(|\uparrow\rangle + i|\downarrow\rangle)/\sqrt{2}$, and (c) $|\downarrow\rangle$; these states are defined on a rotating frame with a frequency δ_g determined by the bias magnetic field. At $t = 0$ ms, we begin transporting single nuclear spins from the MOT to the cavity with the moving lattice. At $t = 50$ ms, the nuclear spin is polarized to the down state using the spin polarization beam (399 nm). Superposition states are created by applying the $\pi/2$ pulse at (a) $t = 100.0$ ms and at (b) $t = 100.1$ ms. To reconstruct the density matrix ρ for each state, we perform projective measurements for the single nuclear spins along three directions. To perform the projective measurements along three orthogonal axes, we rotate the spins using Rabi oscillation or Larmor precession techniques before irradiating the atoms with the pump beam. Figure 3 shows the density matrix ρ for each state reconstructed by using the maximum-likelihood estimation method. The purity ($p = \mathrm{Tr}[\rho^2]$) and the fidelity to the ideal state ($f = \langle\psi_i|\rho|\psi_i\rangle$, where $|\psi_i\rangle$ is the ideal state) are estimated to be (a) $(p, f) = (0.98 \pm 0.01, 0.99 \pm 0.005)$, (b) $(p, f) = (0.96 \pm 0.01, 0.98 \pm 0.005)$ and (c) $(p, f) = (0.97 \pm 0.03,\ 0.98 \pm 0.02)$; the Monte Carlo method is employed for this estimation by assuming a binomial distribution for the signal counts. The purities and fidelities for Fig. 3 are slightly less than 1 and are limited by the distortion of the rf field and photon scattering due to the moving lattice. One-way quantum computing requires a highly efficient projective measurement because the computation is based on the result of individual projection and the scalability is therefore determined by the detection efficiency. Fast and

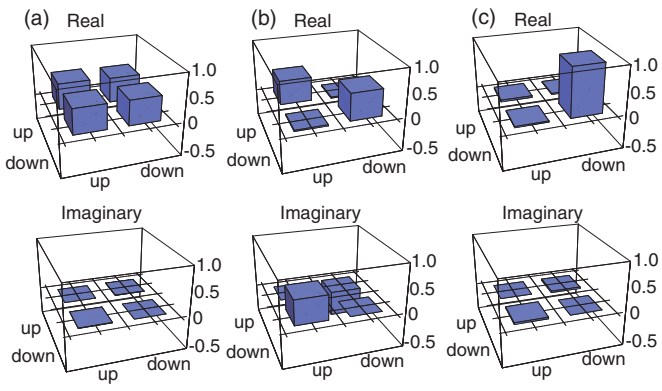

FIG. 3. (Color online) Full quantum state tomography. Real and imaginary parts of density matrices for the prepared nuclear spin states reconstructed using the maximum likelihood estimation. The corresponding spin states are (a) $(|\uparrow\rangle + |\downarrow\rangle)/\sqrt{2}$, (b) $(|\uparrow\rangle + i|\downarrow\rangle)/\sqrt{2}$, and (c) $|\downarrow\rangle$.

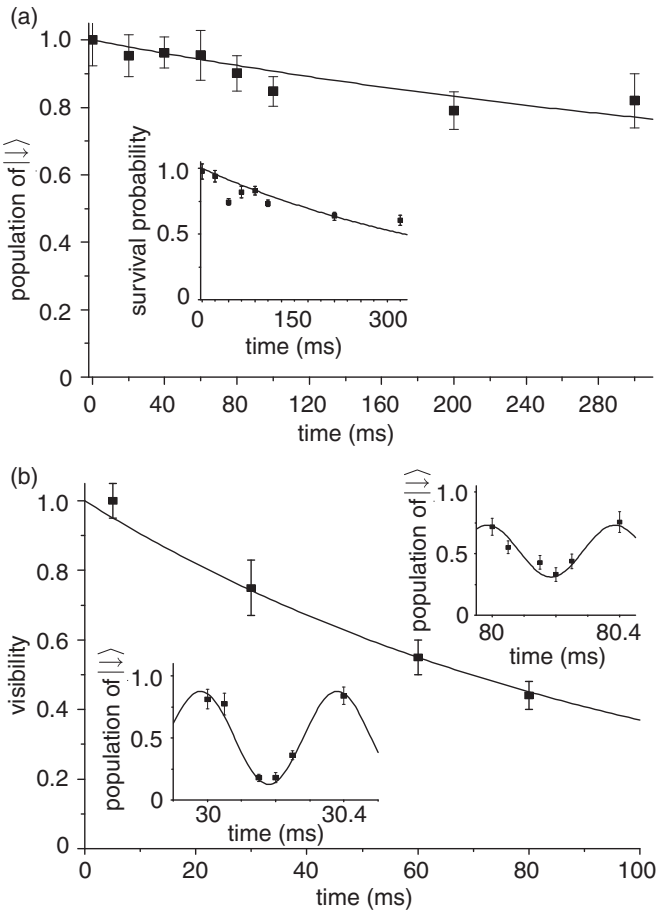

FIG. 4. Measurement of coherence time of single nuclear qubit. (a) Decay of population of $|\downarrow\rangle$ state. The inset shows the survival probability of an atom in the cavity as a function of time. (b) Time development of visibility of Ramsey fringe. The inset shows typical examples of Ramsey interference patterns. For both cases (a) and (b), the error bars are evaluated on the basis of the binomial distribution of signal counts.

efficient detection are realized in our experiment by using the hyperfine interaction and also the enhanced mode-selective spontaneous emission due to the Purcell effect derived from the cavity QED system [7]. Although the detection efficiency is determined by the photon-count rate [(4 counts)/(500 μs)] in our experiment, a dramatic improvement (0.9998) can be expected by simply collecting atomic fluorescence from both sides of the cavity. Such an extremely high value of efficiency will help in performing thousands of operations in one-way quantum computing.

To evaluate the longitudinal relaxation time T_1, we first measure the lifetime τ of single Yb atoms in the microcavity mode. We prepare the spin state of $|\downarrow\rangle$ and measure the population of $|\downarrow\rangle$ as a function of the trapping time. Next, the spin state $|\uparrow\rangle$ is prepared, and the dependence of the population of $|\downarrow\rangle$ on the trapping time is measured. The sum of them gives the survival probability of single Yb atoms in the microcavity mode as a function of the trapping time [see inset of Fig. 4(a)]; the lifetime τ is estimated to be 0.44 ± 0.03 s by fitting the data to an exponentially decaying function. Figure 4(a) shows the population of $|\downarrow\rangle$ as a function of the trapping time; the fitting is

obtained by normalizing the population of $|\downarrow\rangle$ with the survival probability. From the fit, the longitudinal relaxation time T_1 is estimated to be 0.49 ± 0.15 s. To estimate the transverse relaxation time T_2, we measure the visibility of the Ramsey interference as a function of the trapping time [Fig. 4(b)]. The insets of Fig. 3(b) show typical Ramsey interferences, where the horizontal axis represents the time separation between two rf pulses and the vertical axis represents the population of the down-spin state. The transverse relaxation time T_2 is estimated to be 0.10 ± 0.01 s from the fit. It should be noted that, in the case of neutral alkali atoms, the coherence time of Zeeman sublevels is only of the order of 10 μs [8]. Even in the case in which both the clock states of different hyperfine substates and the spin echo technique are used, the coherence time is limited to 30 ms [11]. The coherence time of 0.1 s obtained in our experiment is thus much longer than that of alkali atoms. Here, we discuss the possible sources responsible for the decoherence. The experimentally obtained values of T_1 and T_2 are limited by photon scattering due to the moving lattice and by the fluctuation or inhomogeneity of the bias magnetic field. Because the fluctuation of the bias magnetic field does not affect the population of the spin state, T_1 is considered to be determined by the photon scattering rate Γ_p according to the relation $T_1 = 1/\Gamma_p$. The photon scattering rate Γ_p is estimated to be 2.0 s^{-1} from the experimental parameters, including the imperfection of the mode match of counterpropagating beams. The inverse of Γ_p is 0.5 s which is in agreement with the experimentally obtained value of $T_1 = 0.49$ s. Here, we define the decoherence rate Γ_m, which originates from the energy-conserving dephasing effect due to the fluctuation and inhomogeneity of the bias magnetic field. Because transverse relaxation occurs due to longitudinal relaxation and the dephasing effect, the relation $1/T_2 = 1/T_1 + \Gamma_m$ should be satisfied. From the experimentally obtained values of T_1 and T_2, Γ_m is estimated to be 8 s^{-1}, which corresponds to the magnetic field fluctuation of 9 mG. The ratio of T_2 and the time required for the projective measurement is 200. The suppression of the magnetic field fluctuation below 1 mG is technically possible; suppression to such values will increase the coherence time to values up to 0.5 s.

In this article, we manipulate the single nuclear spin qubit of a Ytterbium atom by using an optical lattice and conveyor belt technique and construct a cavity QED system with a trapped single nuclear spin qubit. In the cavity we perform a spin rotation with NMR and high fidelity control of the single nuclear spin. We also observe the coherence time of the single nuclear spin qubit, and it is few order of magnitude larger than other electronic spin systems [8,11]. Note that a cluster state can be created for the nuclear spin qubits of neutral atoms by using an ultranarrow optical transition such as $^1S_0 \rightarrow {}^3P_2$, since laser detuning avoiding spontaneous emission can be much smaller than the hyperfine splitting. Such a condition cannot be realized in the case of alkali-metal atoms. It will also be possible to implement a randomized benchmarking of a quantum gate with the current setup [12].

We would like to thank M. Takeuchi, N. Takei, P. Zhang, T. Mukaiyama, T. Kishimoto, and S. Inouye for their stimulating and fruitful discussions.

[1] I. Reichenbach and I. H. Deutsch, Phys. Rev. Lett. **99**, 123001 (2007).
[2] L. Jiang *et al.*, Phys. Rev. Lett. **100**, 073001 (2008).
[3] A. J. Daley, M. M. Boyd, J. Ye, and P. Zoller, Phys. Rev. Lett. **101**, 170504 (2008).
[4] K. Shibata *et al.*, Appl. Phys. B **97**, 753 (2009).
[5] A. V. Gorshkov *et al.*, Phys. Rev. Lett. **102**, 110503 (2009).
[6] R. J. Schoelkopf and S. M. Girvin, Nature (London) **451**, 664 (2008).
[7] J. Bochmann, M. Mucke, C. Guhl, S. Ritter, G. Rempe, and D. L. Moehring, Phys. Rev. Lett. **104**, 203601 (2010).
[8] W. Rosenfeld, S. Berner, J. Volz, M. Weber, and H. Weinfurter, Phys. Rev. Lett. **98**, 050504 (2007).
[9] M. Takeuchi *et al.*, Phys. Rev. A **81**, 062308 (2010).
[10] N. Takei *et al.*, Phys. Rev. A **81**, 042331 (2010).
[11] M. P. A. Jones *et al.*, Phys. Rev. A **75**, 040301(R) (2007).
[12] E. Knill *et al.*, Phys. Rev. A **77**, 012307 (2008).